Cell Reports, Volume *22*

Supplemental Information

Genetic Ablation of miR-33 Increases Food Intake, Enhances Adipose Tissue Expansion, and Promotes Obesity and Insulin Resistance

Nathan L. Price, Abhishek K. Singh, Noemi Rotllan, Leigh Goedeke, Allison Wing, Alberto Canfrán-Duque, Alberto Diaz-Ruiz, Elisa Araldi, Ángel Baldán, Joao-Paulo Camporez, Yajaira Suárez, Matthew S. Rodeheffer, Gerald I. Shulman, Rafael de Cabo, and Carlos Fernández-Hernando

SUPPLEMENTAL INFORMATION

MATERIALS AND METHODS

Animals

Male C57BL/6 (*WT*) mice were purchased from The Jackson Laboratory (Bar Harbor, ME, USA) and kept under constant temperature and humidity in a 12 h controlled dark/light cycle. Generation of *miR-33*$^{-/-}$ mice was accomplished with the assistance of Cyagen Biosciences Inc. CRISPR/Cas9 mediated excision of miR-33 was accomplished using targeted guide sequences toward intron 16 of the *Srebp-2* gene. The success of this approach has been verified by Southern blotting and confirmed by PCR based genotyping using specific primers. All mice were fed a standard chow diet for 8-10 weeks after which were either switched to a high fat diet (60% calories from fat: Research Diets D12492) for 1-20 weeks or maintained on chow diet. For fasting-refeeding experiments mice were fasted for 24 h beginning at 8:00am or fasted for 24 h beginning at 8:00pm followed by 12 h of feeding overnight. All of the experiments were approved by the Institutional Animal Care Use Committee of Yale University School of Medicine.

Hyperinsulinemic-euglycemic clamp studies

Hyperinsulinemic-euglycemic clamps were performed in chronically catheterized awake mice as previously described (Jurczak et al., 2012). A jugular venous catheter was implanted 6 to 7 d before the studies were performed. To assess basal whole-body glucose turnover, [3-^{3}H]-glucose (HPLC purified) (PerkinElmer Life Sciences, Waltham, MA, USA) was infused at a rate of 0.05 μCi/min for 120 min into the jugular catheter after with-holding food overnight. After the basal period, hyperinsulinemic-euglycemic clamps were conducted for 140 min with a 4-min primed infusion of insulin [10 mU/(kg-min)] and [3-^{3}H]-glucose (0.24 μCi/min), followed by a continuous [2.5 mU/(kg-min)] infusion of human insulin (Novolin; Novo Nordisk, Bagsværd, Denmark) and [3-^{3}H]-glucose (0.1 μCi/min), and a variable infusion of 20% dextrose. A 10- μCi bolus of 2-deoxy-d-[1-^{14}C] glucose (PerkinElmer) was injected after 85 min to

determine insulin-stimulated tissue glucose uptake. Plasma samples were obtained from the tip of the tail at 0, 25, 45, 65, 80, 90, 100, 110, 120, 130, and 140 min. The tail cut was made at least 2 h before the first blood sample was taken to allow for acclimatization, according to standard operating procedures. Mice received an intravenous artificial plasma solution (115 mM NaCl, 5.9 mM KCl, 1.2 mM $MgCl_2$-$6H_2O$, 1.2 mM NaH_2PO_4-H_2O, 1.2 mM Na_2SO_4, 2.5 mM CaCl-$2H_2O$, 25 mM $NaHCO_3$, and 4% BSA [pH 7.4]) at a rate of 4.2 ml/min during the insulin-stimulated period of the clamp to compensate for volume loss secondary to blood sampling. At the end of the clamps, mice were anesthetized with sodium pentobarbital injection (150 mg/kg), and all tissues taken were freeze-clamped in liquid nitrogen and stored at -80°C for subsequent use.

Lipoprotein profile and lipid measurements

Mice were fasted for 12–16 h overnight before blood samples were collected by retro-orbital venous plexus puncture, and plasma was separated by centrifugation. HDL-C was isolated by precipitation of non-HDL-C and both HDL-C fractions and total plasma were stored at -80°C. Total plasma cholesterol and TAGs were enzymatically measured (Wako Pure Chemicals Tokyo, Japan) according to the manufacturer's instructions. The lipid distribution in plasma lipoprotein fractions were assessed by fast performed liquid chromatography gel filtration with 2 Superose 6 HR 10/30 columns (Pharmacia Biotech, Uppsala, Sweden).

Fat Tolerance Test

Fat tolerance test (FTT) was performed as previously described (Gordts et al., 2016). Briefly, mice were fasted for 4 h beginning at 7:00 am, followed by oral gavage of 10 μL olive oil / gram of BW. Blood samples were collected from the tail vein 0, 1, 2, 4, and 6 h after administration.

Tissue lipid uptake

Determination of lipid uptake in tissues was performed as previously described (Kotas et al., 2013). Briefly, mice were fasted for 6 h beginning at 7:00am. 1 h prior to administration, emulsion mixture was prepared by desiccation of 2μCi [H^3]-Trioline, addition of 100μL of mouse intralipid 20% emulsion oil, and sonication on ice for 10 min at 100 W, 0.5 pulse mode to generate micelles. 2 h after administration by oral gavage, mice were euthanized and plasma/tissues collected (heart, liver, kidney, WAT, BAT, and muscle). 100-150 mg pieces of each tissue were weighed using a precision balance and lipids were extracted with isopropyl alcohol-hexane (2:3;v/v). The lipid layer was collected, evaporated and [^{3}H]-cholesterol radioactivity measured by liquid scintillation counting.

***Ex vivo* lipolysis**

In vitro adipose explant lipolysis assays were performed as previously described (Schweiger et al., 2014). Briefly, ~20 mg of epididymal adipose tissue explants were incubated for 2 h at 37°C in DMEM containing 2% fatty acid -free BSA with or without 10uM Isoproterenol. Medium samples were collected to assay for fatty acids using Wako NEFA-C-kit according to the manufacture's protocol. The level of free fatty acid was normalized to the weight of adipose explants.

Adipocyte size and precursor analysis

For adipocyte size quantification, and CD68 staining, perigonadal adipose tissue was fixed in zinc-formalin, mounted in paraffin blocks, cut into 5 micron sections and stained with Hemotoxylin/Eosin, or CD68 (Bio-Rad MCA1957). The area of each adipocyte (in square pixels) was measured using CellProfiler image analysis software (Broad Institute). At least 300 adipocytes were measured for each data point. For adipocyte precursor analysis, flow cytometry samples were processed and analyzed as previously described (Jeffery et al., 2015). In brief, mice were administered 0.8 mg/mL BrdU in their drinking water. Adipose tissue was harvested and digested in Hank's Balanced Salt Solution (Sigma H8264) containing 3% BSA and 0.8 mg/mL Collagenase Type 2 (Worthington Biochemical LS004176) for 75 min in a shaking water bath at 37˚C. Cells were then stained with CD45 APC-eFluor780

(eBioscience, 47-0451-80), CD31 PE-Cy7 (eBioscience, 25-0311-82), CD29 Alexa Fluor 700 (BioLegend, 102218), Sca-1 Pacific Blue (BD Biosciences, 560653). Cells were washed, then fixed with Phosflow Lyse/Fix (BD Bioscience 558049) for 10 min at 37˚C and permeabilized with Perm Buffer III (BD Bioscience 558050) on ice for 30 min. The cells were then incubated in DNase I (Worthington Biochemical LS002007) for 90 min at 37˚C and stained in anti-BrdU antibody (Phoenix Flow Systems AX647) overnight at 4˚C. Finally, the cells were washed and stained with the previously mentioned antibodies (CD45, CD31, CD29, and Sca-1) in addition to CD34 PE (119307) and CD24 PerCp Cyanine 5.5 (eBioscience, 45-0242,80). Cells were washed and analyzed using a BD LSRII analyser. Data was analyzed using BD FACS Diva software (BD Biosciences).

Body composition and metabolic cage analysis

Analysis of body composition was performed by Echo MRI (Echo Medical System). A Comprehensive Lab Animal Monitoring System (CLAMS; Columbus Instruments, Columbus, OH, USA) was used to evaluate O_2 consumption, CO_2 production, energy expenditure, activity, and food consumption.

Monitoring of food intake and pair feeding

For evaluation of food intake and pair feeding experiments mice were separated into individual cages at least 4 days prior to experiments. For determination of daily food intake mice were fed a known amount of HFD and the remaining food was measured between 4:00 and 5:00pm daily. For pair feeding experiments mice were begun one day after ad libitum fed animals and animals were provided HFD between 4:00 and 5:00 pm based on the average food intake of ad libitum fed wildtype mice the day before.

Glucose tolerance test (GTT)

Glucose tolerance tests (GTT) were performed by IP injection of glucose at a dose of 2g/kg for chow diet and 1g/kg for ad libitum HFD fed mice and 1.5g/kg for pair fed mice. Blood glucose was

measured at 0, 15, 30, 60, and 120 min post injection.

Measurement of circulating hormones

Circulating hormones were measured by ELISA according to manufacturer's instructions: Insulin (CrystalChem #90080), Leptin (Abcam, ab100718), Ghrelin (Novus Biologicals, KA1863), Corticosterone (Alpco, 55-CORMS-E01), and FGF21 (RD Systems MF2100).

Western blot analysis.

Tissues were homogenized by manual disruption and the Bullet Blender Homogenizer. Both tissues and cells were lysed in ice-cold buffer containing 50 mM Tris–HCl, pH 7.5, 0.1% SDS, 0.1% deoxycholic acid, 0.1mM EDTA, 0.1mM EGTA, 1% NP-40, 5.3 mM NaF, 1.5 mM NaP, 1 mM orthovanadate and 1 mg/ml of protease inhibitor cocktail (Roche), and 0.25 mg/ml AEBSF (Roche). Lysates were sonicated and rotated at 4°C for 1 h before the insoluble material was removed by centrifugation at 12,000 × *g* for 10 min. After normalizing for equal protein concentration, cell lysates were resuspended in SDS sample buffer before separation by SDS–PAGE. Following transfer of the proteins onto nitrocellulose membranes, the membranes were probed with the following antibodies: anti-ATGL (Cell Signaling, #2138, 1:1000), anti-HSL (Cell Signaling #4107, 1:1000), anti-HMGA2 (Biocheck, #59170AP, 1:1000), anti-FASN (Cell Signaling #31895), anti-ACC (Cell Signaling #3662) and anti-HSP90 (BD Biosciences, #610419, 1:1000). For SREBP-1 processing blots liver lysates were homogenized with a dounce homogenizer in SREBP lysis buffer: Tris-HCl 20mM pH 8, KCl 120 mM, DTT 1mM, EGTA 2mM, Triton X-100 0.1%, Nonidet P40 al 0.5%, protease inhibitors, NaF 100 mM, Na_2MoO_4 20 mM, β-glycerophosphate 20 mM, Na_3VO_4 2 mM, PMSF 1 mM and caspase-3 inhibitor Ac-DMQD-CHO (alexis) and probed with an anti-SREPB-1 antibody (Santa Cruz SC-13551). Protein bands were visualized using the Odyssey Infrared Imaging System (LI-COR Biotechnology) and densitometry was performed using ImageJ software. For Western blot analysis of ApoA1 (Abcam, #20453, 1/1000) in lipoprotein fractions,

an equal volume of three fractions were mixed with reducing SDS sample buffer and separated as described above.

For Western blot analysis of ApoB100 and ApoB48 in pooled lipoprotein fractions, separation was performed on a NuPAGE Novex 4-12% Tris-Acetate Mini Gel using 1x NuPAGE Tris-Acetate SDS running buffer (Invitrogen). Following overnight transfer of proteins onto nitrocellulose membranes, the membranes were blocked in 5% (w/v) non-fat milk dissolved in wash buffer. The membranes were probed with an antibody against ApoB (Meridian, #K23300R, 1:2000) overnight at 4°C and visualized as above.

PKC translocation assay.

PKC translocation was assessed in the livers of mice that were fasted for 6 h for HFD animals and fed overnight for CD. Membrane-associated and cytosolic fractions were prepared as previously described (Petersen et al., 2016). After normalizing for equal protein concentration, cell lysates were resuspended in reducing SDS sample buffer and separated on 4%-12% Tris-glycine gels (Novex). Following a 2 h semi-dry transfer onto PVDF membranes (Immunobilon-P; EMD Millipore), the membranes were blocked in 5% (w/v) non-fat dry milk or 5% (w/v) BSA dissolved in wash buffer according to manufacturer's recommendations. Membranes were probed overnight at 4°C with the following primary antibodies diluted in blocking solution: PKCε (1:1000; BD610086), GAPDH (1:5000; Cell Signaling 5174), and Na-K ATPase (1:1000; Abcam ab7671). Membranes were then washed in TBS-T and incubated for 1 h at room temperature with HRP-conjugated secondary antibodies (Cell Signaling Technology) diluted in blocking buffer. After further washing in TBS-T, antibody binding was visualized by enhanced chemiluminescence (Pierce). Films were developed at multiple exposures and images within the linear dynamic range of signal intensity were scanned for digital analysis. Densitometry analysis of the gels was carried out using ImageJ software from the NIH (http://rsbweb.nih.gov/ij/). The ratio of membrane PKC intensity (normalized to Na-K ATPase intensity) to cytosolic PKC intensity (normalized to GAPDH intensity) was calculated.

Liver lipid measurements.

Mice were fasted 6 h before liver collection for HFD fed animals and fed overnight for CD. Liver triglycerides were extracted by the method of Bligh and Dyer (Bligh and Dyer, 1959) and measured using a colorimetric assay (Sekisui). Liver diacylglycerols were extracted from cytosolic/lipid droplet and membrane-associated fractions and measured by LC-MS/MS essentially as described (Galbo et al., 2013; Yu et al., 2002). Total diacylglycerols are reported as the sum of individual species. Liver ceramides were extracted and measured by LC-MS/MS according to previously established methods.

RNA isolation and quantitative real-time PCR

Total RNA from tissue was isolated using TRIzol reagent (Invitrogen) according to the manufacturers protocol. For mRNA expression analysis, cDNA was synthesized using iScript RT Supermix (Bio-Rad), following the manufacturers protocol. Quantitative real-time PCR (qRT-PCR) analysis was performed in duplicate using SsoFast EvaGreen Supermix (BioRad) on an iCycler Real-Time Detection System (Eppendorf). The mRNA levels were normalized to 18S.

Microarray Analysis

Microarray analysis was performed as previously described (Fang et al., 2017). Briefly, 200 ng of total RNA was labeled using the Agilent Low-Input QuickAmp Labeling Kit and hybridized onto Agilent SurePrint G3 Mouse 8x60K Microarray (Agilent Technologies) using the Gene Expression Hybridization Kit (Agilent Technologies). Following post-hybridization rinses, arrays were scanned using an Agilent Agilent Microarray Scanner (Agilent Technologies). Data extraction and quality control fulfillment was performed using Agilent's Feature Extraction Software. Qlucore Omics Explorer v 3.2 (Qlucore AB, Lund, Sweden) was used for identifying differentially-expressed genes ($P < 0.01$) using a one-way analysis of variance (ANOVA) or a two-tailed t-test comparison. Principal component analysis plots, unsupervised hierarchical clustering, and heat maps were also generated in Qlucore. Ingenuity Pathway Analysis (Ingenuity Systems QIAGEN, Content version: 33559992, 2017, Redwood City, CA, USA) was used to

carry out analyses for pathway, network, and molecular and cellular functions for differentially-expressed genes across samples. Each gene symbol was mapped to its corresponding gene object in the Ingenuity Pathways Knowledge Base. Networks of these genes are algorithmically generated based on their connectivity and assigned a score. The score is a numerical value used to rank networks according to how relevant they are to the genes in the input dataset but may not be an indication of the quality or significance of the network. The over-represented cellular and molecular functions and networks were ranked according to the calculated P-value.

Circulating leukocyte analysis

Blood was collected by retro-orbital puncture in heparinized microhematocrit capillary tubes. Measurement of total circulating numbers of blood leukocytes was performed using a HEMAVET system. For further FACs analysis, erythrocytes were lysed with ACK lysis buffer (155 mM ammonium chloride, 10 mM potassium bicarbonate, and 0.01 mM EDTA, pH 7.4). White blood cells were resuspended in 3% fetal bovine serum in PBS, blocked with 2 mg/ml FcgRII/III, then stained with a cocktail of antibodies. Monocytes were identified as $CD115^{hi}$ and subsets as Ly6-C^{hi} and Ly6-C^{lo}. The following antibodies were used (all from BioLegend, San Diego, CA, USA): FITC-Ly6-C (AL-21), PE-CD115 (AFS98), and APC-Ly6-G (1A8).

Short-term lipid absorption studies

10-weeks old WT and *miR-33*$^{-/-}$ mice fed a CD were fasted overnight and injected i.p. with poloxamer 407 (25 mg/mouse). 1 h after the injection, mice were gavaged with 5 μCi of [^{3}H]-triolein in 25 μL of olive oil. 30, 60 and 120 min after the injection, the plasma was isolated for measurement of radioactivity in 40 μL.

Statistical analysis

Animal sample size for each study was chosen based on literature documentation of similar well-characterized experiments. The number of animals used in each study is listed in the figure legends. In vitro experiments were routinely repeated at least three times unless otherwise noted. No inclusion or exclusion criteria were used and studies were not blinded to investigators or formally randomized. Data are expressed as average ± SEM. Statistical differences were measured using an unpaired two-sided Student's t-test, or one-way ANOVA with Bonferroni correction for multiple comparisons. Normality was checked using the Kolmogorov-Smirnov test. A nonparametric test (Mann-Whitney) was used when data did not pass the normality test. A value of $P \leq 0.05$ was considered statistically significant. Data analysis was performed using GraphPad Prism Software Version 7 (GraphPad, San Diego, CA).

SUPPLEMENTAL REFERENCES

Bligh, E.G., and Dyer, W.J. (1959). A rapid method of total lipid extraction and purification. Can J Biochem Physiol *37*, 911-917.

Fang, E.F., Waltz, T.B., Kassahun, H., Lu, Q., Kerr, J.S., Morevati, M., Fivenson, E.M., Wollman, B.N., Marosi, K., Wilson, M.A., et al. (2017). Tomatidine enhances lifespan and healthspan in C. elegans through mitophagy induction via the SKN-1/Nrf2 pathway. Sci Rep *7*, 46208.

Galbo, T., Perry, R.J., Jurczak, M.J., Camporez, J.P., Alves, T.C., Kahn, M., Guigni, B.A., Serr, J., Zhang, D., Bhanot, S., et al. (2013). Saturated and unsaturated fat induce hepatic insulin resistance independently of TLR-4 signaling and ceramide synthesis in vivo. Proc Natl Acad Sci U S A *110*, 12780-12785.

Gordts, P.L., Nock, R., Son, N.H., Ramms, B., Lew, I., Gonzales, J.C., Thacker, B.E., Basu, D., Lee, R.G., Mullick, A.E., et al. (2016). ApoC-III inhibits clearance of triglyceride-rich lipoproteins through LDL family receptors. The Journal of clinical investigation *126*, 2855-2866.

Jeffery, E., Church, C.D., Holtrup, B., Colman, L., and Rodeheffer, M.S. (2015). Rapid depot-specific activation of adipocyte precursor cells at the onset of obesity. Nat Cell Biol *17*, 376-385.

Jurczak, M.J., Lee, A.H., Jornayvaz, F.R., Lee, H.Y., Birkenfeld, A.L., Guigni, B.A., Kahn, M., Samuel, V.T., Glimcher, L.H., and Shulman, G.I. (2012). Dissociation of inositol-requiring enzyme (IRE1alpha)-mediated c-Jun N-terminal kinase activation from hepatic insulin resistance in conditional X-box-binding protein-1 (XBP1) knock-out mice. J Biol Chem *287*, 2558-2567.

Kotas, M.E., Jurczak, M.J., Annicelli, C., Gillum, M.P., Cline, G.W., Shulman, G.I., and Medzhitov, R. (2013). Role of caspase-1 in regulation of triglyceride metabolism. Proceedings of the National Academy of Sciences of the United States of America *110*, 4810-4815.

Petersen, M.C., Madiraju, A.K., Gassaway, B.M., Marcel, M., Nasiri, A.R., Butrico, G., Marcucci, M.J., Zhang, D., Abulizi, A., Zhang, X.M., et al. (2016). Insulin receptor Thr1160 phosphorylation mediates lipid-induced hepatic insulin resistance. J Clin Invest *126*, 4361-4371.

Schweiger, M., Eichmann, T.O., Taschler, U., Zimmermann, R., Zechner, R., and Lass, A. (2014). Measurement of lipolysis. Methods in enzymology *538*, 171-193.

Yu, C., Chen, Y., Cline, G.W., Zhang, D., Zong, H., Wang, Y., Bergeron, R., Kim, J.K., Cushman, S.W., Cooney, G.J., et al. (2002). Mechanism by which fatty acids inhibit insulin activation of insulin receptor substrate-1 (IRS-1)-associated phosphatidylinositol 3-kinase activity in muscle. J Biol Chem *277*, 50230-50236.

Figure S1

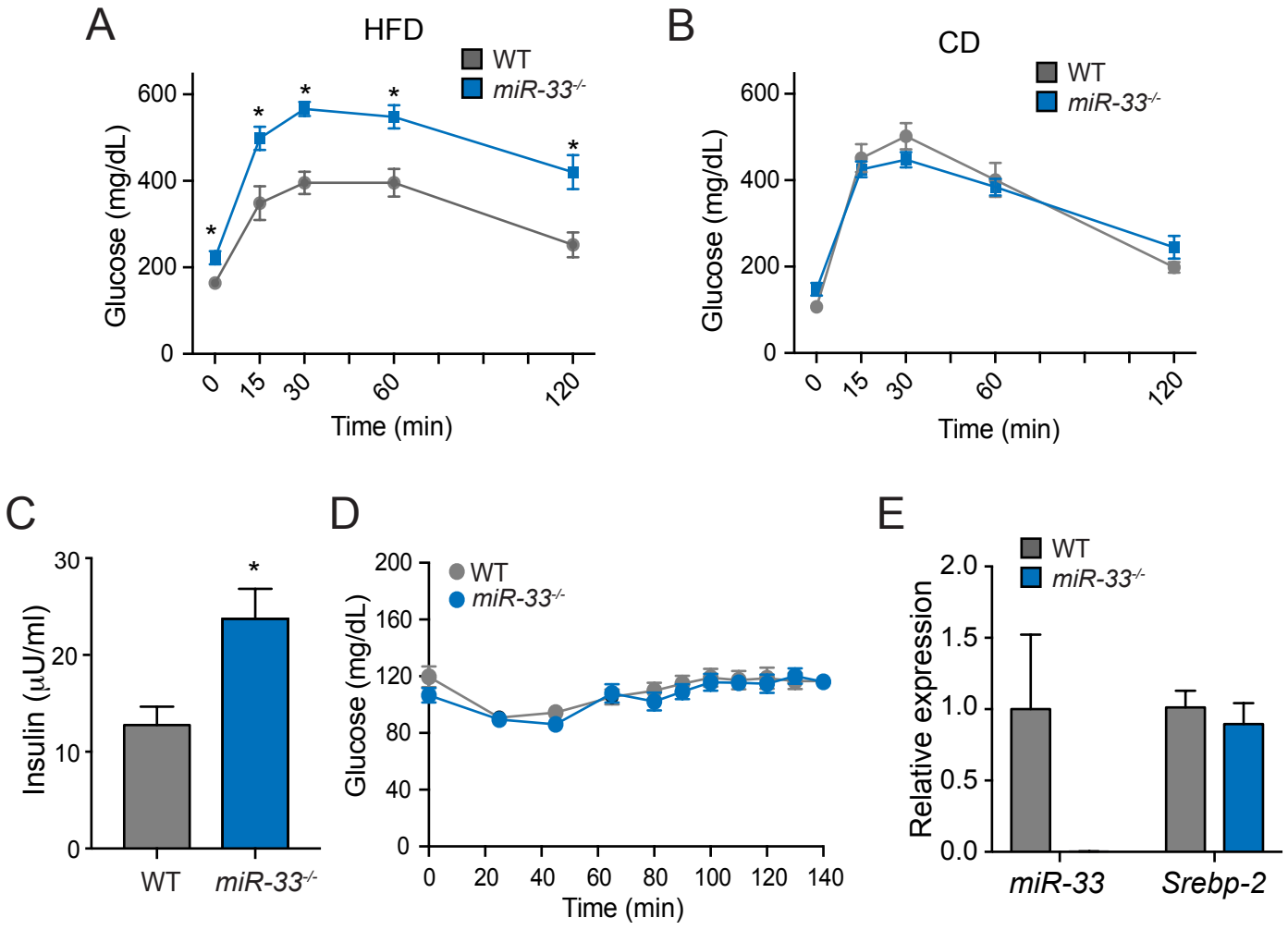

Figure S1. Genetic ablation of miR-33 disrupts glucose homeostasis in high fat diet fed mice without affecting *Srebp-2* expression. Related to Figures 1 and 2.

(**A** and **B**) Glucose tolerance test (GTT) in WT and *miR-33*$^{-/-}$ mice fed a high fat diet (HFD) (**A**) or chow diet (CD) (**B**) for 11 weeks (n=6-7). (**C**) Circulating insulin in WT and *miR-33*$^{-/-}$ mice fed a CD for 20 weeks (n=9). (**D**) Circulating glucose levels during the hyperinsulinemic euglycemic clamp studies. (**E**) qRT-PCR analysis of miR-33 expression and *Srebp-2* mRNA expression in the livers of WT and *miR-33*$^{-/-}$ animals (n=3). All data represent the mean±SEM and * indicates $P < 0.05$ comparing*miR-33*$^{-/-}$ with WT mice.

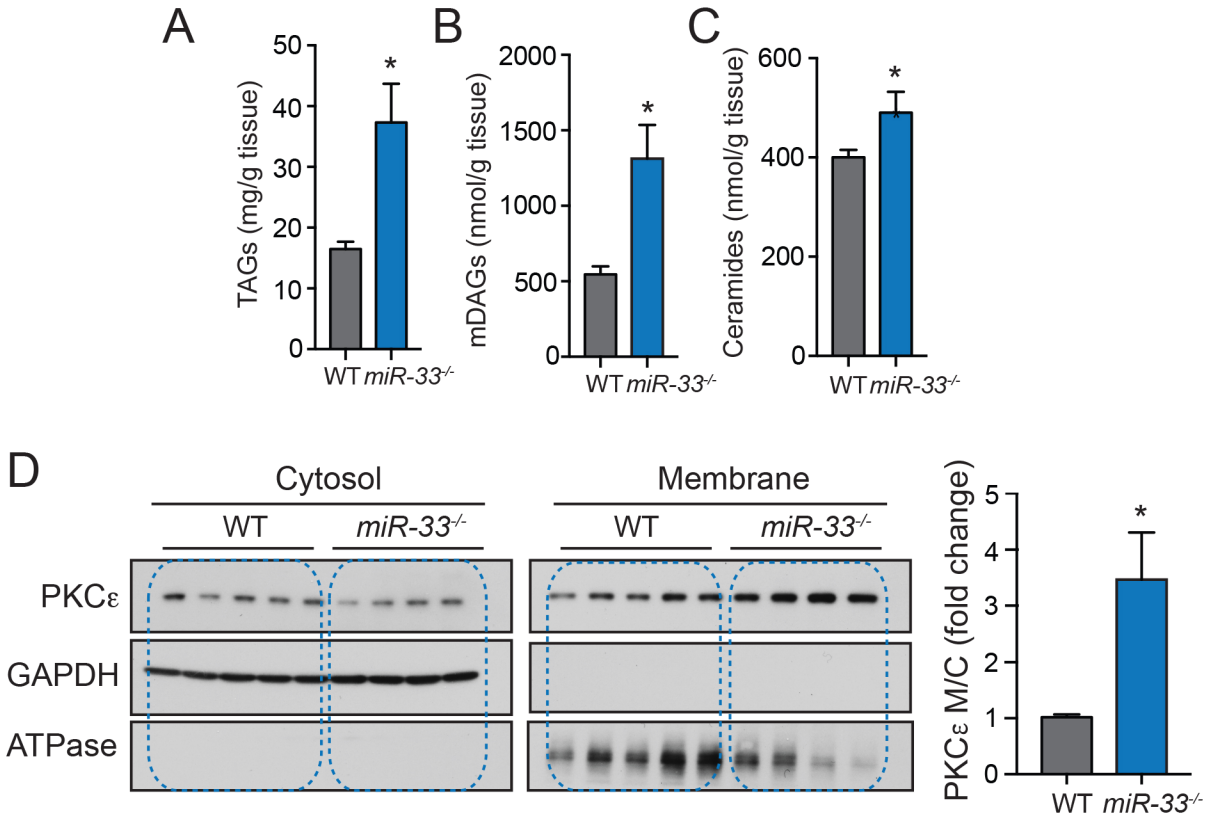

Figure S2. Loss of miR-33 increases liver triglyceride, diacylglycerol and ceramide content and reduces PKCε activation. Related to Figure 3.
(**A-C**) liver triglyceride (TAG) (**A**), diacylglycerol (DAG) (**B**) and ceramide (**C**) content in WT and *miR-33*$^{-/-}$ mice fed a high fat diet (HFD) for 8 weeks and fasted for 6 h. (n=9-10). (**D**) Western blot analysis of PKCε translocation in WT and *miR-33*$^{-/-}$ mice fed a HFD for 8 weeks and fasted for 6 h. Quantification is shown in right panels (n=9-10). GAPDH and ATPase were used as loading controls for cytosolic and membrane fractions respectively. All data represent the mean ±SEM and * indicates $P < 0.05$ comparing *miR-33*$^{-/-}$ with WT mice on the same diet.

Figure S3

A

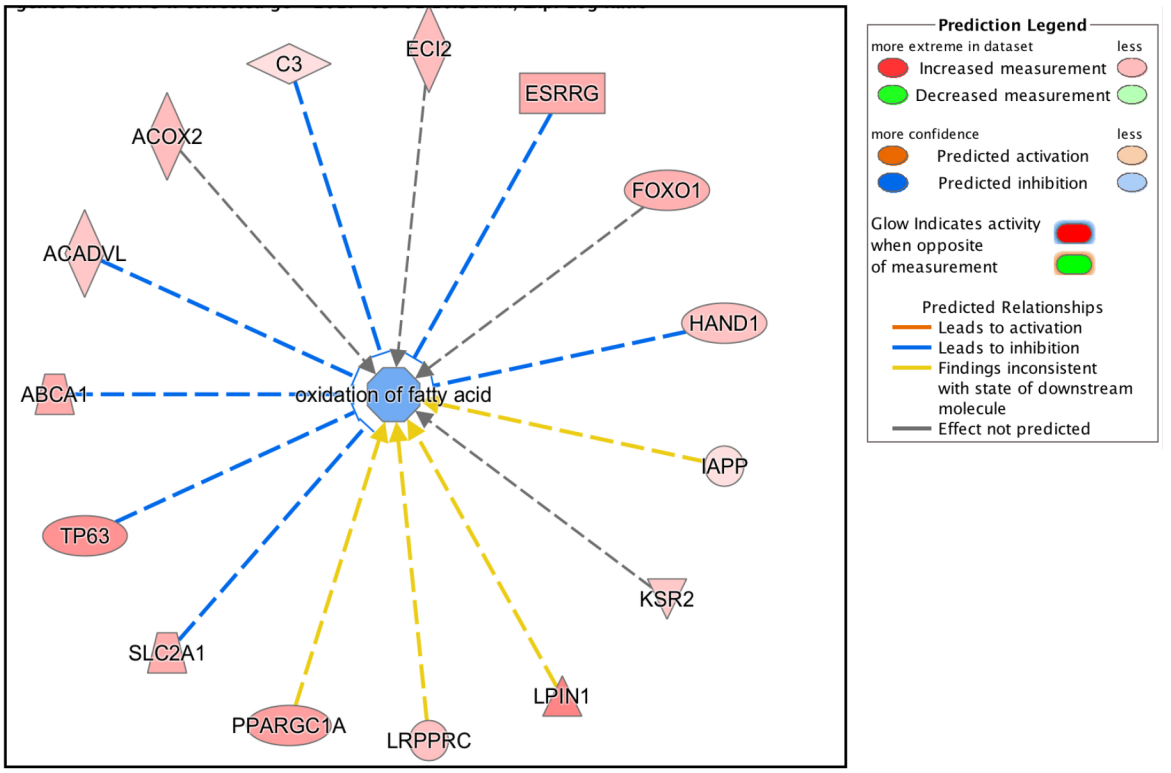

B

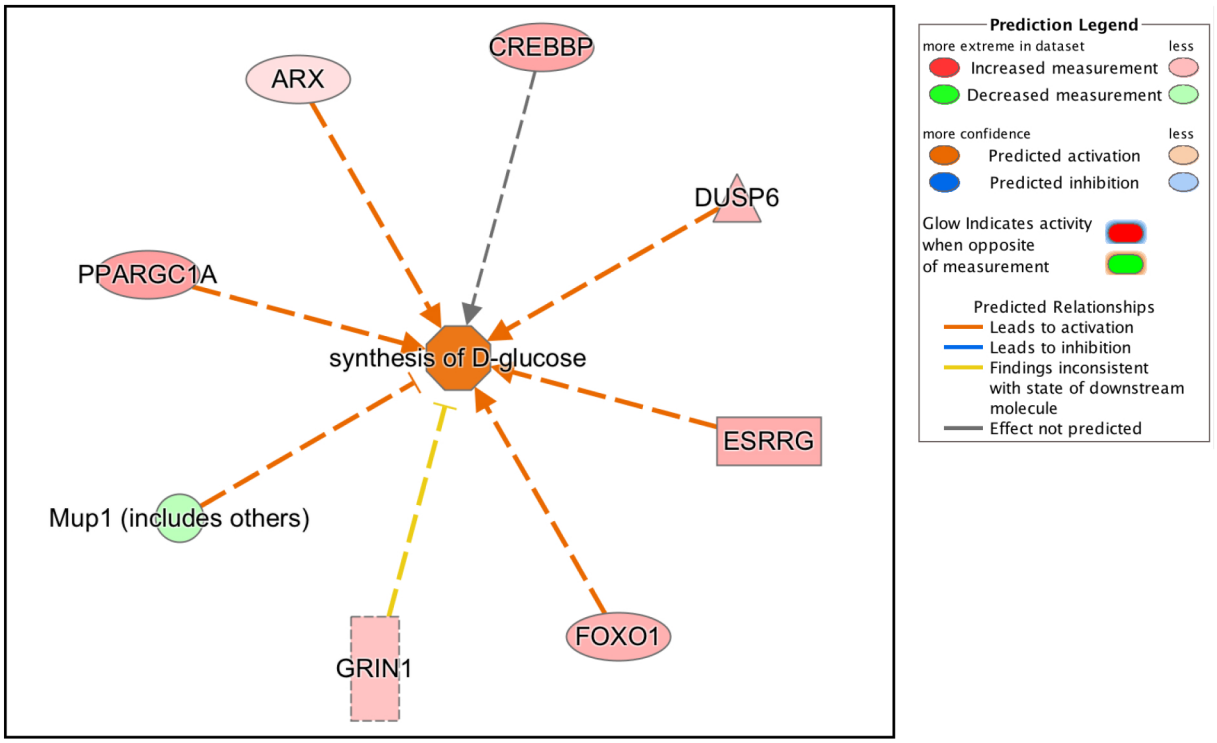

Figure S3. Absence of miR-33 does not impact protein levels of SREBP-1 target genes but does impair insulin regulatory effects on fatty acid oxidation and gluconeogenesis in miR-33$^{-/-}$ mice fed a HFD. Related to Figure 4.
(**A** and **B**) Assessment of cellular and molecular functions altered in livers of miR-33 deficient mice using Ingenuity Pathway Analysis (IPA) bioinformatics tool identified oxidation of fatty acids (**A**) and synthesis of glucose (**B**) as two of the most significantly altered functions. Genes represented in green are down-regulated and genes in red are up-regulated (P > .01) in liver samples isolated from fed *miR-33*$^{-/-}$ mice on a high fat diet (HFD) for 20 weeks compared to liver samples obtained from WT mice.

Figure S4

A

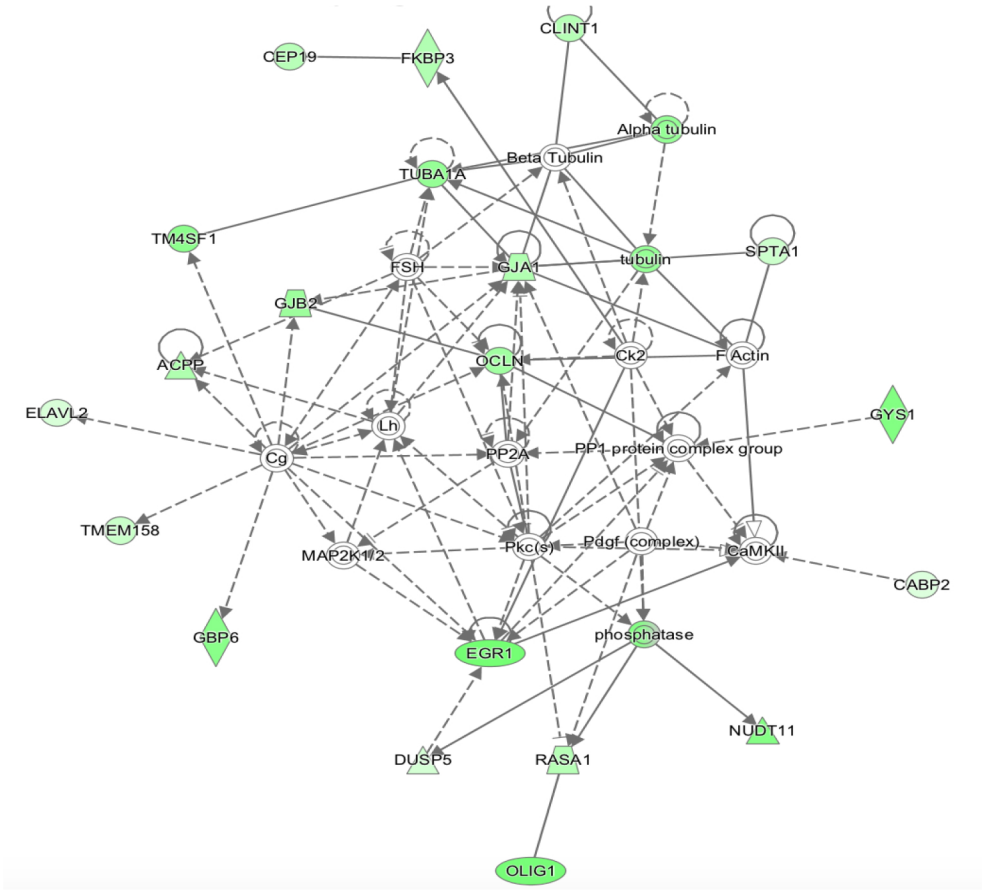

B

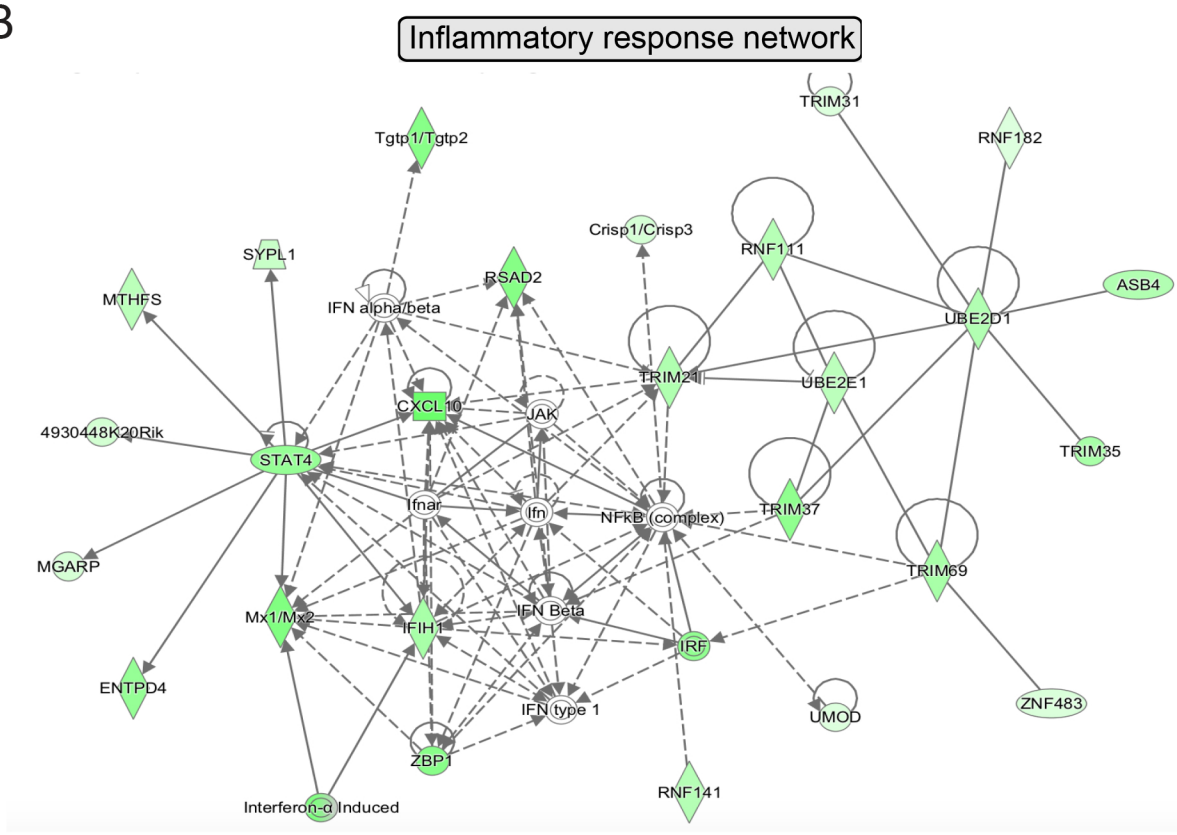

Figure S4. Loss of miR-33 reduces the expression of genes related to liver cholestasis and inflammatory response in the liver of HFD fed mice. Related to Figure 4.

(**A** and **B**) Ingenuity Pathway Analysis (IPA) bioinformatics tool identified hepatic disease and liver cholestasis network (**A**) and inflammatory response network (**B**) among the most highly altered gene networks in *miR-33*$^{-/-}$ mice. Genes represented in green color are down-regulated (P > .01) in liver samples isolated from fasted *miR-33*$^{-/-}$ fed a HFD for 20 weeks compared to liver samples obtained from WT mice.

Figure S5

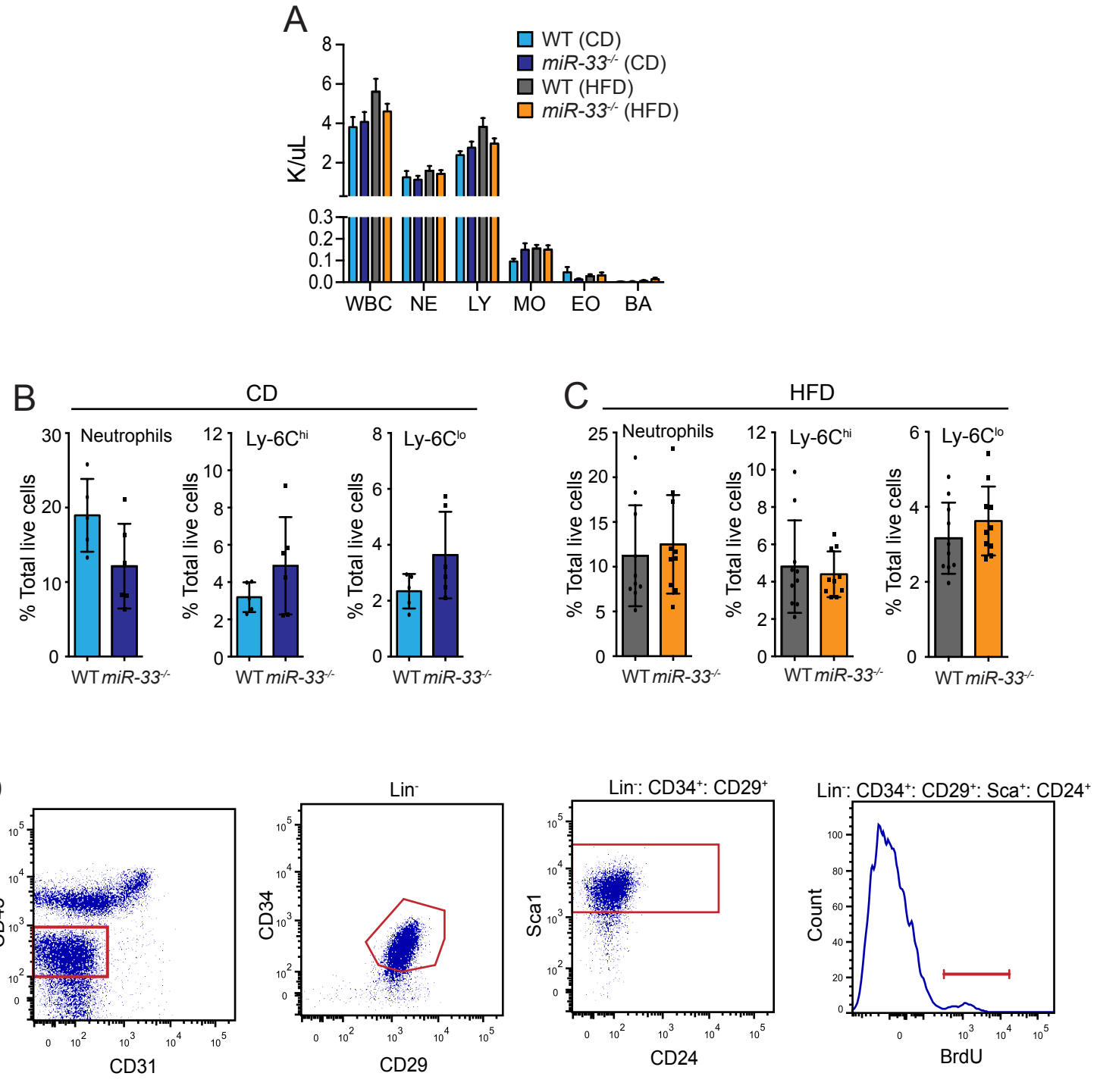

Figure S5. Absence of miR-33 does not influence circulating leukocytes in mice fed a CD or HFD. Related to Figure 5. (**A**) Peripheral blood counts from WT and *miR-33*$^{-/-}$ mice fed a chow diet (CD) or high fat diet (HFD) for 20 weeks measured using Hemavet hematology analyzer. (n=5-6 for CD and n=10 for HFD). (**B** and **C**) Flow cytometry analysis of circulating leukocytes from WT and *miR-33*$^{-/-}$ mice fed a CD (**B**) or HFD (**C**) for 20 weeks. Data is expressed as % of live cells (n=5-6 for CD and n=10 for HFD). All data represent the mean±SEM. (**D**) Dot plot analysis of adipocyte precursors (AP) and BrdU incorporation.

Figure S6

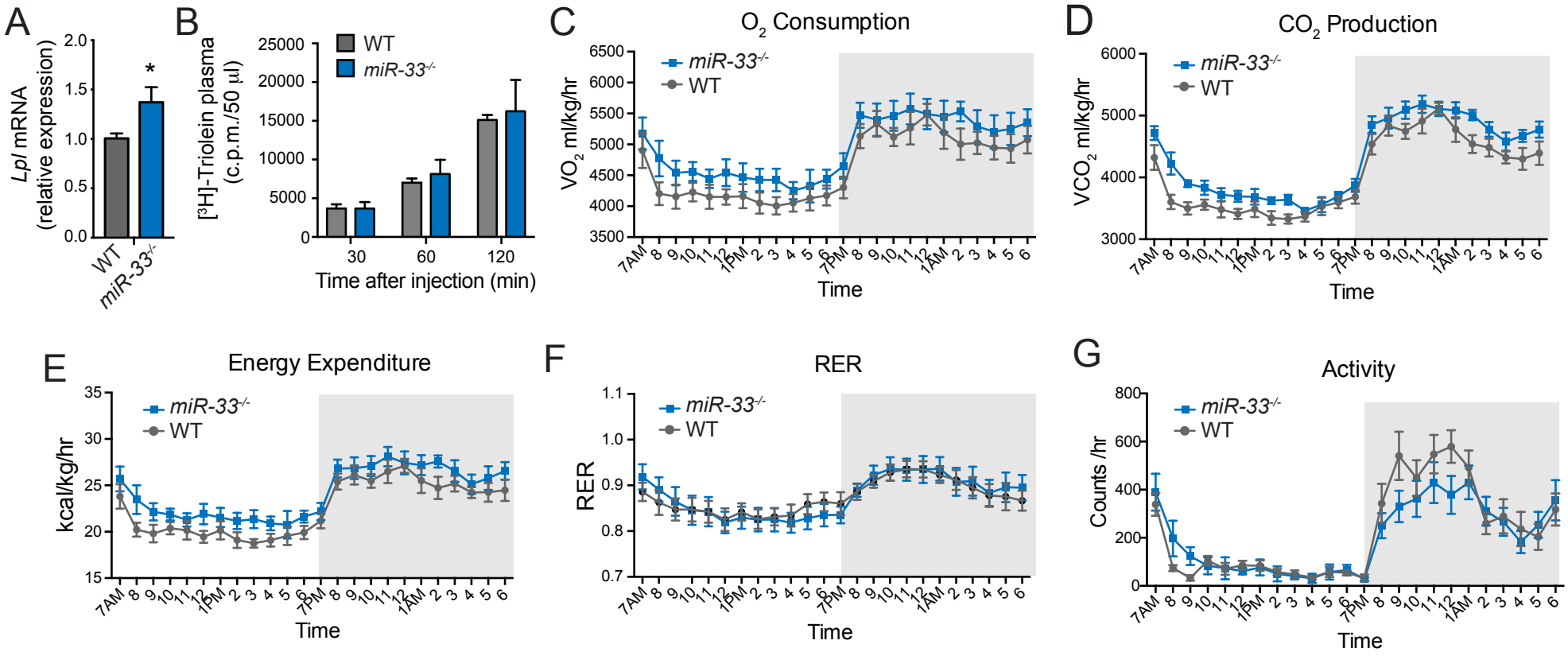

Figure S6. Absence of miR-33 does not affect oxygen consumption, carbon dioxide production and fat absorption but increases LPL expression in WAT. Related to Figures 5 and 6.

(**A**) qRT-PCR analysis of *Lpl* mRNA expression in WAT samples isolated from WT and *miR-33*$^{-/-}$ mice fed a HFD for 1 week. Data represent relative expression levels normalized WT animals (n=6). (**B**) Plasma c.p.m content in WT and *miR-33*$^{-/-}$ mice gavaged with [^{3}H]-Triolein and treated with LPL inhibitor (Poloxamer 407) for the indicated times. (n=4). All data represent the mean±SEM and * indicates $P < 0.05$ comparing *miR-33*$^{-/-}$ with WT mice. (**C**-**G**) Metabolic cage analysis of oxygen consumption (**C**) carbon dioxide production (**D**) respiratory exchange ratio (RER) (**E**), energy expenditure (**F**), and activity (**G**) in WT and *miR-33*$^{-/-}$ mice fed a CD for 20 weeks (n=5-6).

Figure S7

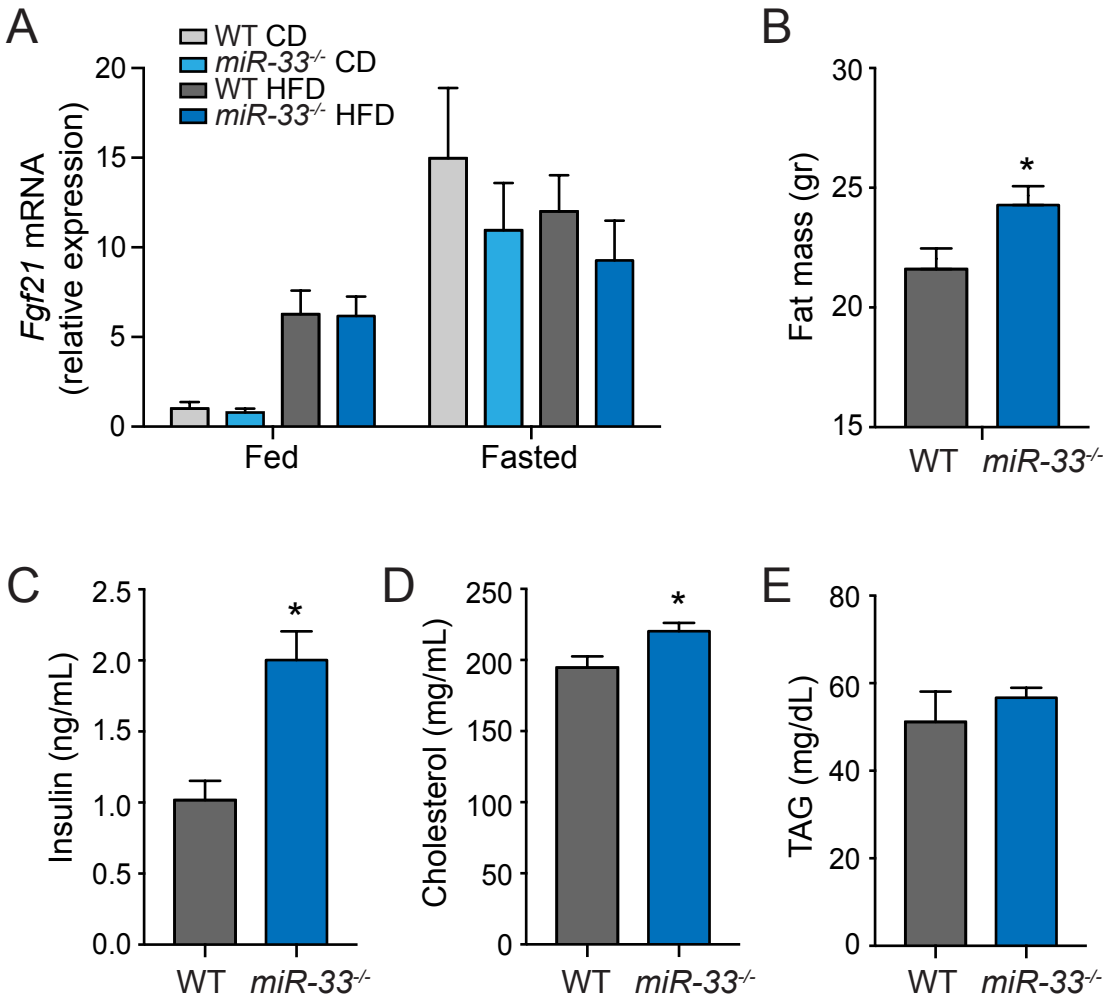

Figure S7. Loss of miR-33 does not impact mRNA expression of FGF21 in the liver, but does cause increased fat mass, and elevated levels of circulating insulin, cholesterol and TAGs after 12 weeks high fat diet feeding. Related to Figure 6.

(**A**) qRT-PCR analysis of *Fgf21* mRNA expression in liver samples isolated from WT and *miR-33*$^{-/-}$ mice fed a chow diet (CD) or high fat diet (HFD) for 20 weeks. Data represent relative expression levels normalized fed WT animals on CD (n=6-11). (**B**) Fat mass of WT and *miR-33*$^{-/-}$ mice fed HFD ad libitum for 12 weeks (n=7-10). (**C**-**E**) circulating levels of insulin (**C**), cholesterol (**D**) and triglycerides (TAG) (**E**) in plasma of WT and *miR-33*$^{-/-}$ mice fed HFD ad libitum for 12 weeks after overnight fasting (n=10). All data represent the mean±SEM and * indicates $P < 0.05$ comparing *miR-33*$^{-/-}$ with WT mice.